CSR wakefields: latest results and remaining problems

Gennady Stupakov
SLAC National Accelerator Laboratory, Menlo Park, CA 94025

LOWeRING 2016, October 26-28, 2016

Outline of the talk

- New results in theory and experiment
- Not yet (fully) solved problems of CSR wakes and instabilities (personal opinion)

A comprehensive review of earlier CSR studies was given by D. Zhou at the TWIICE-2 workshop in February 2016, (`http://www.diamond.ac.uk/Home/Events/2016/TWIICE-2.html`).

Introduction

There are several analytical models of CSR wakefields.
The simplest one is the CSR wake for circular motion in free space[1]. The theory assumes

1. Free space
2. Ultra-relativistic beam, $v = c$ or $\gamma = \infty$.
3. Filament beam, $\sigma_\perp = 0$.

From 2 and 3 it follows that the beam longitudinal profile is frozen and does not change with time.

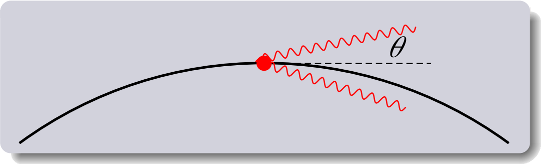

The wake is determined by the radiation at angles $\theta_r \sim (\lambdabar/\rho)^{1/3}$ where ρ is the bending radius, $\lambdabar = \lambda/2\pi \sim \sigma_z$.

[1] Derbenev, Rossbach, Saldin and Shiltsev, DESY FEL Report TESLA-FEL 95-05, (1995); Murphy, Krinsky, and Gluckstern, PAC95 (1995).

CSR for a circular orbit in free space

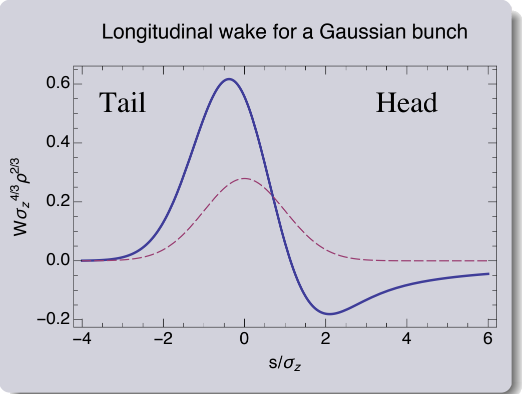

CSR impedance per unit length

$$Z_{\text{vac}}(k) = (1.63+0.94i)\frac{k^{1/3}}{c\rho^{2/3}}$$

$k = \omega/c$.

Positive wake corresponds to the energy loss, negative wake–energy gain.

This plot is universal, all the parameters of the problem (σ_z—the bunch length, ρ—the bending radius) are in the scalings.

Formation length of the wake: $l_\parallel \sim (24\rho^2\sigma_z)^{1/3} \sim \lambda/\theta_r^2$.

CSR for circular orbit with shielding by parallel plates

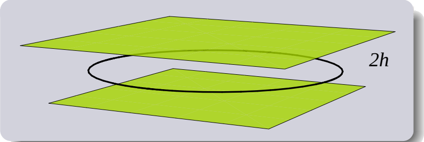

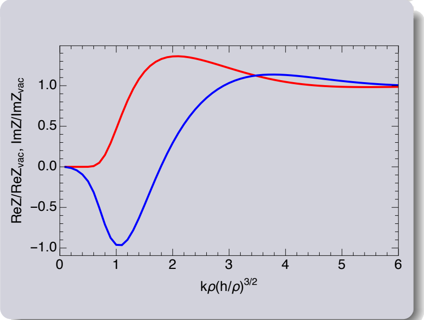

Calculated in the paper by Murphy et al.[2] The same assumptions as before except for the free space.

Plot of $\mathrm{Re}\,Z/\mathrm{Re}\,Z_{\mathrm{vac}}$ (red) and $\mathrm{Im}\,Z/\mathrm{Im}\,Z_{\mathrm{vac}}$ (blue). The wake gets suppressed when $h \lesssim l_\perp = (\lambda^2\rho)^{1/3} \sim \lambda/\theta_r$—the transverse coherence size.

Using this impedance we can calculate the wake of a bunch with given longitudinal charge distrbitution.

[2] J. B. Murphy, S. Krinsky, and R. L. Gluckstern, Part. Accel. 57, 9 (1997).

Difference between CSR problems in rings and linacs

Case 1. In linacs (for FEL applications) we deal with extremely short bunches ($\sim 10 - 100\ \mu$). The shielding in many cases does not play a big role. In bunch compressors, CSR radiation occurs together with beam compression which complicates analysis. CSR causes emittance growth and microbunching of the beam.

Case 2. In rings $\sigma_z \sim 1$ cm. The shielding plays a role: the shape and dimensions of the vacuum chamber may be important. CSR can cause a microwave instability (CSR bursts). Of great interest is the threshold of the instability. In some cases the beam dynamics above the threshold (bursts) is also of interest.

New results in theory and experiment

- Analytical theory of CSR wakefield of short bunches shielded by conducting parallel plates (G. Stupakov and D. Zhou)
- Efficient computation of coherent synchrotron radiation in a rectangular chamber (R. Warnock and D. Bizzozero)
- Recent experimental results from ANKA

Parallel-plates model

In reality we do not have perfectly circular orbits of Murphy et al.[3]—typically we have straight-bend-straight arrangements. Sometimes damping wigglers are used to lower the beam emittance and one needs to know the contribution of CUR to the impedance. In Ref.[4] we extended the analysis for arbitrary trajectories between two parallel conducting plates.

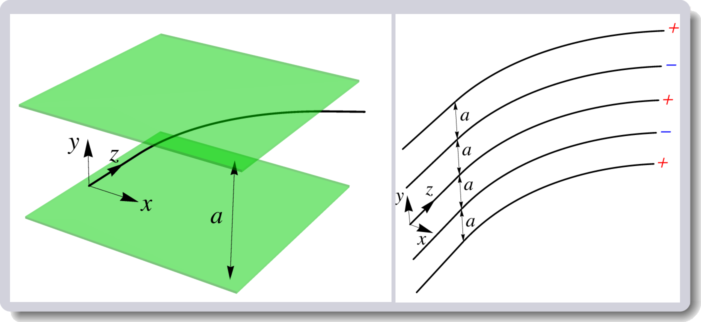

[3] J. B. Murphy, S. Krinsky, and R. L. Gluckstern, Part. Accel. 57, 9 (1997).

[4] G. Stupakov and D. Zhou, PRAB **19**, 044402 (2016).

Parallel-plates model

Assuming $v = c$ a general formula for the CSR impedance can be obtained for short bunches

$$Z(k) = \frac{ik}{c^2} \int_{-\infty}^{\infty} ds \int_{-\infty}^{s} ds' \sum_{m=-\infty}^{\infty} (-1)^m \frac{1 - \boldsymbol{\beta}(s) \cdot \boldsymbol{\beta}(s')}{\tau_m(s, s')} e^{-ik(s-s'-c\tau_m(s,s'))}$$

$$\tau_m = |\mathbf{r}(s) - \mathbf{r}(s') + ma\hat{\mathbf{y}}|$$

In principle, this formula allows to compute the impedance with trajectories that are straight lines at $\pm\infty$. The summation should be carried out first, before the integration. However, a better convergence is achieved through rearranging the summation.

Wakes known in literature and new wakes

Using the new formula we reproduced CSR wakes known in the literature:

- 1. Circular orbit in free space
- 2. Circular orbit between two parallel metallic plates
- 3. Infinitely long wiggler with $K \gg 1$ in free space[5]

and obtained new results

- CSR impedance of a kink (short, strong magnet)
- CSR impedance of a bend of finite length
- Impedance of a finite length undulator

All new results are benchmarked agains the computer code CSRZ that calculates CSR radiation in a vacuum chamber of rectangular cross section.[6]

[5] J. Wu, T. Raubenheimer, and G. Stupakov, Phys. Rev. ST Accel. Beams **6**, 040701 (2003).

[6] D. Zhou, Ph.D. thesis, Department of Accelerator Science, The Graduate University for Advanced Studies, 2011.

Wiggler of infinite length—comparison with CSRZ

We calculated the radiation impedance for NSLS-II damping wigglers[7]: $N_w = 70$, $\lambda_w = 10$ cm, $K = 16.8$. The beam energy is 3 GeV, $\theta_0 = 1.86 \times 10^{-3}$, $a = 11.5$ mm. In the simulations the horizontal size $b = 3a$.

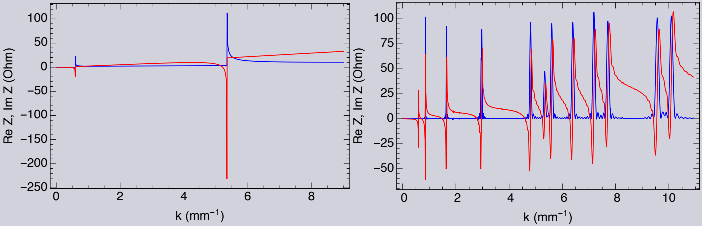

The impedance is dominated by the resonances with the waveguide modes[8]

$$k - k_w = \sqrt{k^2 - \frac{\pi^2 n^2}{a^2} - \frac{\pi^2 m^2}{b^2}}$$

where n is an odd and m is an even number.

[7] http://www.bnl.gov/nsls2/project/PDR, BNL (2007).

[8] G. Stupakov and D. Zhou, Preprint SLAC-PUB-14332, SLAC (2010).

Comparison of the wake for the NSLS-II wiggler

Using the impedance we computed the wake for a short bunch $\sigma_z = 0.5$ mm—black is analytical theory, blue is the CSRZ wake with $b/a = 3$ and magenta is the CSRZ wake with $b/a = 16$.

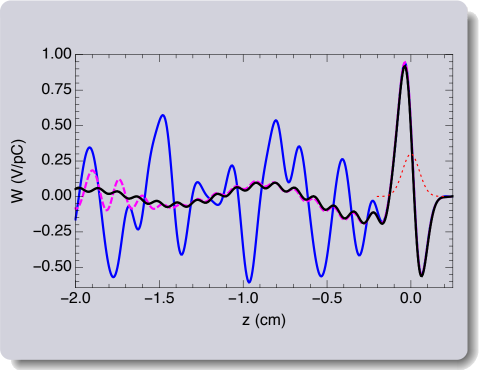

New CSR code from Warnock and Bizzozero

There are several codes that solve CSR radiation in a vacuum chamber with rectangular geometry.

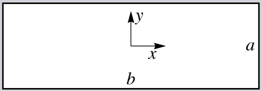

They use either discretized equations on the mesh[9] or eigenmode expansion[10]. R. Warnock and D. Bizzozero have recently developed a new code that combines both approaches[11]. They used the parabolic equation (the SVA approximation) combined with the mode expansion in y and a mesh in x.

$$F(s,x,y,t) = \int_{-\infty}^{\infty} dk e^{ik(s-\beta ct)} \sum_{p=0}^{\infty} \begin{pmatrix} \sin(\pi p(y/a+1/2)) \\ \cos(\pi p(y/a+1/2)) \end{pmatrix} \hat{F}_p(k,s,x)$$

where $F = E_s,\ E_x,\ H_y,\ J_s,\ J_x,\ \rho,\ H_s,\ H_x,\ E_y,\ J_y$.
In the horizontal direction the beam distribution is $\propto \delta(x)$-function. The ODE equations on the horizontal mesh are numerically solved along s. The authors applied the new approach to calculation of the wake and the rw energy loss for LCLS-II bending magnet in a bunch compressor.

[9] T. Agoh and K. Yokoya, PRST-AB, **7**, 054403 (2004); K. Oide, PAC09 (2009); D. Zhou, Ph.D Thesis (2011); .

[10] G. Stupakov and I. Kotelnikov, PRST-AB, **12**, 104401 (2009).

[11] R. Warnock, D. Bizzozero, PRAB, **19**, 090705 (2016).

New CSR code from Warnock and Bizzozero

Rectangular vacuum chamber with $a = 2$ cm, $b = 5$ cm, bending radius $R = 12.9$ m, bend angle $\theta = 42.5$ mrad, $Q = 100$ pC. The longitudinal bunch distribution is taken from LCLS-II simulations.

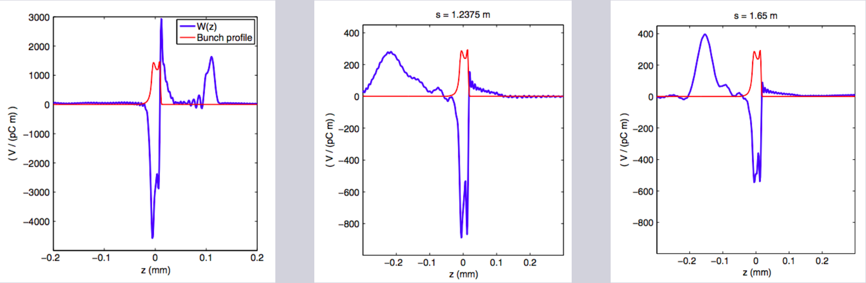

Left—wake field $W(z, s)$ as a function of $z = s - \beta ct$ at $s = 0.55$ m (end of bend); center—at $s = 1.23$ m; right— at $s = 1.65$ m.

The CSR radiation is eventually absorbed in the wall due to the resistivity.

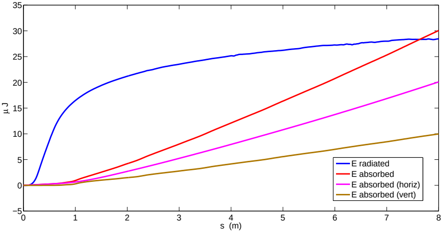

The total energy radiated in perfectly conducting model (blue); energy absorbed in the walls (red); energy absorbed in horizontal walls (magenta); energy absorbed in vertical walls (brown). The beginning of the bend is at $s = 0$, where the fields have the steady-state values for an infinite straight waveguide.

CSR instability—experiment vs theory

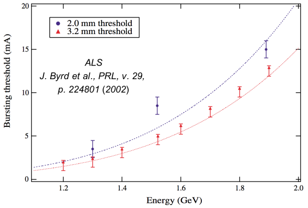

FIG. 4 (color online). Bursting threshold as a function of electron beam energy at 3.2 and 2 mm wavelengths. Data are shown as points. Calculated threshold using nominal ALS parameters at 3.2 and 2 mm wavelengths are shown as dashed lines.

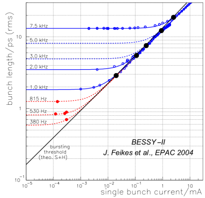

Figure 2: Measured bunch length as a function of the current, indicated by colored dots. Blue: streak camera data and empirical fit to the data; black: bursting threshold of coherent THz signals; red: coherent THz radiation based data. At the fitted data lines the rf-voltage amplitude and f_s are indicated.

Experimental result from ALS and BESSY-II

Experimental result from ANKA and CLS

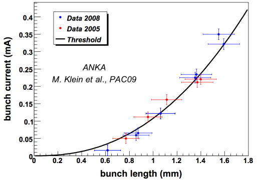

Figure 5: The observed bursting stable threshold as function of bunch current and bunch length. The black curve shows the fit to to the microbunching theory.

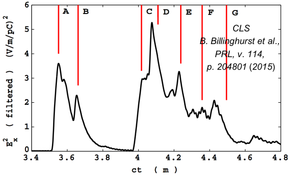

FIG. 5 (color online). Simulated E_x^2 at backward port vs ct, after a low pass filter to account for detector response. The origin of time t is when the bunch is 5 cm before the entrance to the bend. Only the lowest mode in y is included.

Recent ANKA results

Recent results from ANKA[12] demonstrate very good agreement of the bursting threshold with the theory. The experiment used a state-of-the-art bunch-by-bunch feedback system to generate custom filling patterns and high-repetition-rate data acquisition systems.

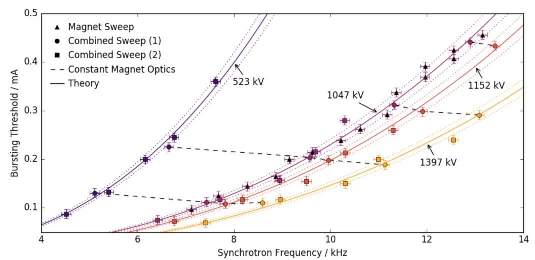

[12] M. Brosi et al. arXiv:1605.00536, (2016).

Threshold of CSR instability

The ANKA experiment is benchmarked agains the theoretical model[13]. The model assumes CSR shielding with parallel plates with a gap $2h$.

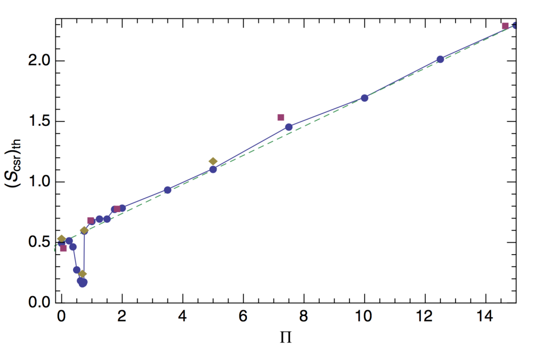

Here $S_{CSR} = I\rho^{1/3}\sigma_z^{4/3}$, $I = r_e N_b / 2\pi\nu_{s0}\gamma\sigma_{\delta 0}$ and $\Pi = \rho^{1/2}\sigma_{z0}/h^{3/2}$.

[13] K. Bane, Y. Cai, G. Stupakov. PRAB, 13, 104402 (2010).

Recent ANKA results

Experiments[14] confirm the existence of the stability island.

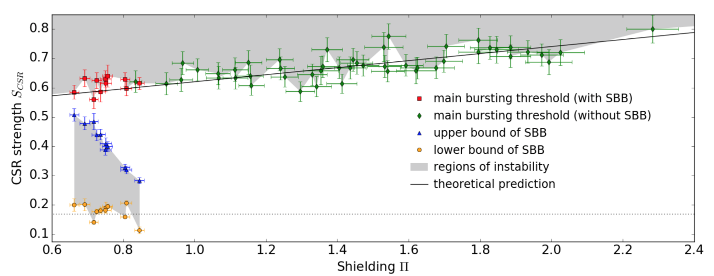

The lower bound (orange discs) as well as the upper bound (blue triangles) of the short bunch-length bursting are shown. The main bursting threshold is shown in red (squares) for machine settings where short bunch-length bursting occurred and in green (diamond) for settings where it did not occur. The error bars display the standard deviation error.

[14] M. Brosi et al. IPAC 2016, paper TUPOR006 (2016).

Three problems that are not yet (properly) solved

- CSR wake for arbitrary geometry of the vacuum chamber
- Compression energy in CSR wakes
- Stability threshold for MWI (driven either by CSR or other wakes)

1. CSR wake for arbitrary geometries

The existing codes almost exclusively assume a rectangular cross section of the vacuum chamber.

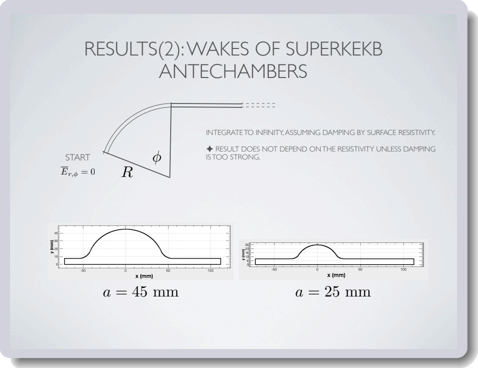

K. Oide tried to develop a code that calculates the CSR wake for more complicated cross sections of the vacuum chamber (invited talk at PAC09). L. Wang from SLAC also worked on a similar code.

A possible approach to this problem may consist of using the mode expansion method in the paraxial approximation

$$\hat{E}_{\perp} = \sum_{p,m} C_{mp}(s)\hat{E}_{mp,\perp}(x, y, s)$$

1. CSR wake for arbitrary geometries

The mode expansion method for calculation of the CSR wakefields inside a vacuum chamber was developed in[15]. The modes in the toroidal waveguide can be found numerically by solving a 2D PDE equation in the cross section of the vacuum chamber.

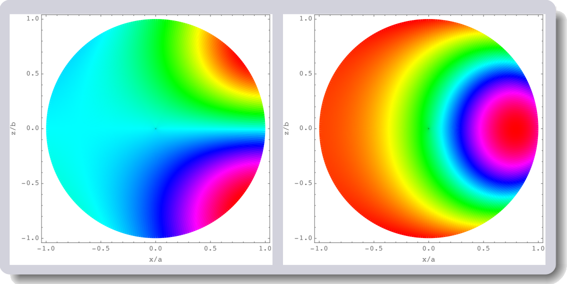

This is especially easy to do if there are analytical expressions for eigenmodes for a straight waveguide of a given cross section (round, elliptical, triangular, etc.).

[15] G. Stupakov and I. Kotelnikov. PRAB **6**, 034401 (2003).

2. Compression work in CSR wakes

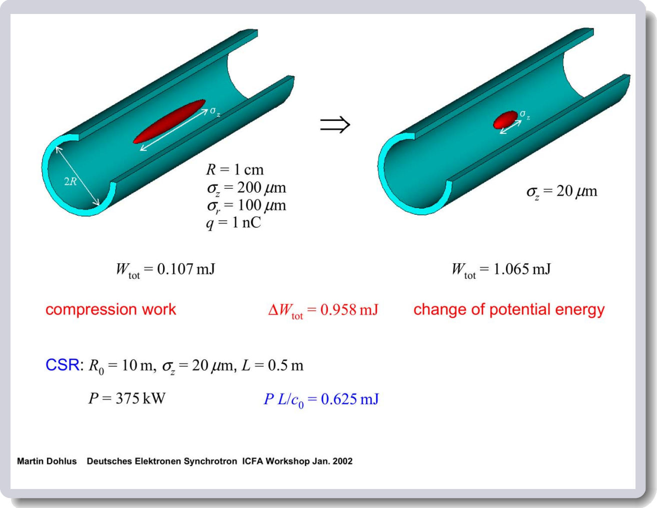

The compression work effect also appears due to variation of the beta-functions and the corresponding change of the transverse size of the beam.

3. Better algorithms for calculations MWI threshold

Simulation of MWI in the FACET-II positron damping ring ($E = 335$ MeV). A short run with artificially large damping time ($\tau_z = 200\ T_s$) seems to show stability (K. Bane's code), while a longer run with realistic damping time ($\tau_z = 1.7 \times 10^4\ T_s$) ends in unstable motion (VFP solver).

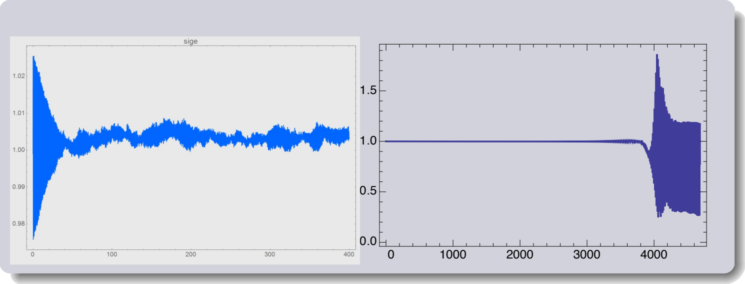

Courtesy K. Bane and Y. Cai.

3. Better algorithms for calculations MWI threshold

To calculate the threshold of the instability one can use the linearized Vlasov equation assuming $\delta F(J,\theta) = f_1(J,\theta)e^{-i\omega t}$. The perturbation of the wake potential $\delta U(J,\theta)$ is

$$\delta U(J,\theta) = e^{-i\omega t} \sum_{n=-\infty}^{\infty} v_n(J)\, e^{in\theta}$$

From the linearized Vlasov equation one finds

$$f_1(J,\theta) = -F_0' \sum_{n=-\infty}^{\infty} \frac{n v_n(J)}{\omega - n\omega_s(J)} e^{in\theta}$$

At the threshold ω is real and $f_1(J,\theta)$ has a singularity when $\omega_s(J) = \omega/n$. In numerical solutions this singular function is approximated with large errors.

The numerical algorithm for threshold calculation that avoids the singularity can be found in[16].

[16] R. Warnock, J. Ellison. EPAC02, p. 1589 (2002); R. Warnock et al. EPAC04, p. 2215 (2004).

Conclusions

- There has been a steady progress in theoretical studies of the CSR impedance and the MWI driven by CSR.
- Remarkable agreement with theory was reported in the latest experiments on ANKA on the threshold of MWI.
- Some long-standing problems still remain: CSR wake for arbitrary cross section of the vacuum chamber; the compression work in CSR wake; fast and reliable method for finding the MWI threshold.